Engineering Notes

ENGINEERING NOTES are short manuscripts describing new developments or important results of a preliminary nature. These Notes cannot exceed 6 manuscript pages and 3 figures; a page of text may be substituted for a figure and vice versa. After informal review by the editors, they may be published within a few months of the date of receipt. Style requirements are the same as for regular contributions (see inside back cover).

A System Analysis View of Aerodynamic Coupling

PETER HAMEL*
Technische Universität Braunschweig, Braunschweig, Germany

Nomenclature†

C_L = lift coefficient
$C_{l\alpha}$ = rolling moment caused by angle of attack, $C_{l\beta\alpha}\beta_o$
$C_{l\beta\alpha}$ = $(\partial C_{l\beta}/\partial\alpha)_{\alpha=\alpha_o}$
$C_{n\alpha}$ = yawing moment caused by angle of attack, $C_{n\beta\alpha}\beta_o$
$C_{n\beta\alpha}$ = $(\partial C_{n\beta}/\partial\alpha)_{\alpha=\alpha_o}$
$C_{m\beta}$ = pitching moment caused by sideslip, $C_{m\beta\beta}\beta_o$
$C_{m\beta\beta}$ = $(\partial^2 C_m/\partial\beta^2)_{\alpha=\alpha_o}$
$L_{\beta\alpha}$ = $\rho S b U_o^2 C_{l\beta\alpha}/2I_x$, 1/sec²
$L_{\beta\alpha}'$ = $[L_{\beta\alpha} + (I_{xz}/I_x)N_{\beta\alpha}]/[1 - I_{xz}^2/I_x I_z]$, 1/sec²
$M_{\beta\beta}$ = $\rho S c U_o^2 C_{m\beta\beta}/2I_y$, 1/sec²
$N_{\beta\alpha}$ = $\rho S b U_o^2 C_{n\beta\alpha}/2I_z$, 1/sec²
$N_{\beta\alpha}'$ = $[N_{\beta\alpha} + (I_{xz}/I_z)L_{\beta\alpha}]/[1 - I_{xz}^2/I_x I_z]$, 1/sec²
U_o = equilibrium true airspeed, m/sec
α_o = equilibrium angle of attack
β_o = steady-state sideslip angle

Introduction

IT is well known to stability and control analysts that various forms of inertial and aerodynamic cross-coupling between longitudinal and lateral flight vehicle motions may exist. In addition, some of the elastic natural vibrations of a flexible flight vehicle can get into the frequency range of flight mechanics and thus cause aeroelastic coupling with the rigid-body motion. It is now in general difficult to indicate the salient features of the stability characteristics of such coupled systems without undertaking extensive numerical computations.

The interest in this Note is focussed on the application of system analysis methods to stability investigations of coupled flight vehicle motions. This point of view is not new and has already been applied to inertial[2] and aeroelastic[3,4] coupling effects. Attention in this Note is drawn to the flight with nonzero steady sideslip angles. The resulting aerodynamic coupling phenomenon has firstly been treated analytically by R. F. Porter and J. P. Loomis[5] and independently by H. Ulke,[6] the latter using a special stability axis system. The important terms of aerodynamic coupling, relevant to sideslip and arising mainly from wing-fuselage interference, are the pitching moment due to sideslip $C_{m\beta}$ and the rolling and yawing moments due to angle of attack $C_{l\alpha}$ and $C_{n\alpha}$. Figure 1 shows typical data for a wing-body combination from six-component balance measurements of Ref. 7.

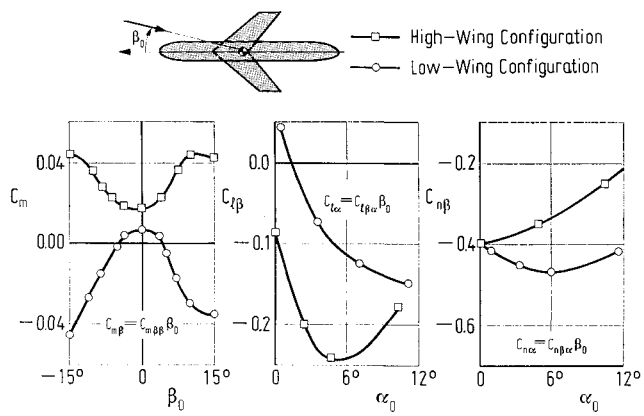

Fig. 1 Effect of wing-fuselage interference on sideslip coupling derivatives.

In the following, the characteristic polynomial of the aerodynamic coupled motion is regarded as a closed-loop characteristic equation of an equivalent feedback system which has an open-loop performance function equal to the ratio of coupling to noncoupled terms. The stability analysis may be treated with standard graphical servo techniques like the root locus method, thus reducing the computational effort to a simple paper and pencil procedure. The relative positions of the singularities (i.e., poles and zeros) of the open-loop performance function, which determine the shape of the root locus branches describe in combination with the root locus, gain the aerodynamic coupling phenomenon. The singularities and the gain acquire simple physical meanings. Parameter influences are achieved by direct variations of the singularities and the gain.

Analysis

The following analysis is based on a set of five-degree-of-freedom perturbation equations. Only the perturbation in forward speed is considered negligible, thus omitting the phygoid mode. The equations of motion were derived using body axes which have the x-axis initially aligned with the flight path. In these equations, the lateral derivatives are primed such as to eliminate the explicit appearance of product-of-inertia coupling terms. Further, it can be shown that the significant aerodynamic coupling between the lateral and longitudinal motion is mainly associated with the three aerodynamic moment derivatives $C_{m\beta}$, $C_{l\alpha}$, and $C_{n\alpha}$ allowing the remaining coupling derivatives due to steady sideslip to be discarded. The characteristic equation of the five-

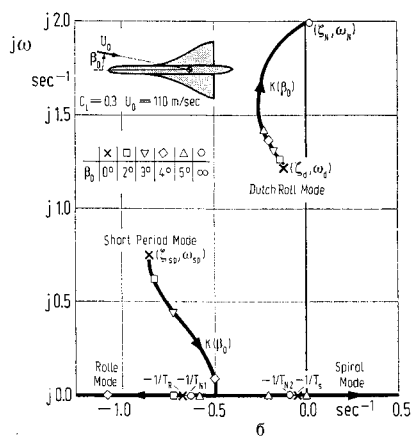

Fig. 2 Variation of the characteristic roots with the steady sideslip angle β_o.

Received April 6, 1970. Author would like to acknowledge Department Head H. Blenk.

* Dr.-Ing., S. M., Lehrstuhl für Flugmechanik.

† The notation used is based, where not specially explained, on the symbols of Ref. 1.

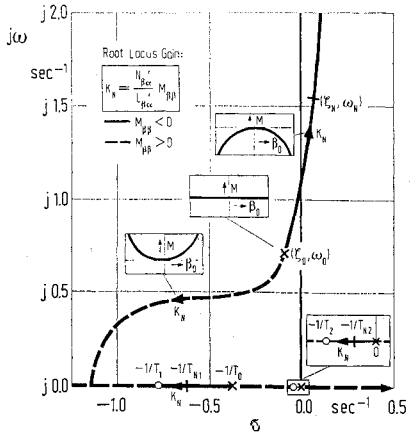

Fig. 3 Effect of the sideslip pitching moment $M_{\beta\beta}$ on the numerator roots (zeros).

degree-of-freedom set can be expanded into a term which shows the uncoupled longitudinal and lateral polynomials in factored form and a coupling polynomial. Transforming this equation into the basic root locus form yields the expression

$$1 + K(\beta_0)\Delta_{coupl}/\Delta_{long}\Delta_{lat} = 0 \quad (1)$$

where the root locus gain

$$K(\beta_0) = L_{\beta\alpha}'\beta_0^2, \quad (2)$$

representing the coupling intensity, is proportional to the square of the sideslip angle, thus, confirming the same coupling effect for either positive or negative sideslip angles. From Eq. (2), it can be further seen that the coupling strength depends directly on the cross-coupling derivative $L_{\beta\alpha}'$.

The roots of the denominator in Eq. (1), describing the "poles" of the equivalent performance function, correspond to the uncoupled longitudinal and lateral motion, hence,

$$\Delta_{long} = s^2 + 2\zeta_{sp}\omega_{sp}s + \omega_{sp}^2 \quad (3)$$

and

$$\Delta_{lat} = (s + 1/T_s)(s + 1/T_R)(s^2 + 2\zeta_d\omega_d s + \omega_d^2) \quad (4)$$

Table 1 summarizes the longitudinal and lateral denominator

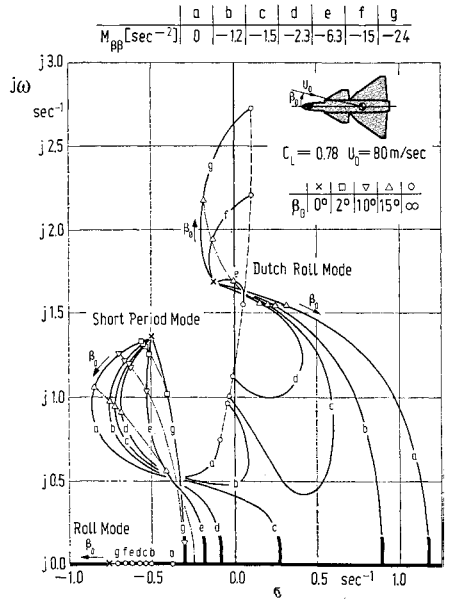

Fig. 4 Variation of the characteristic roots with the steady sideslip angle at various $M_{\beta\beta}$.

Table 1 Denominator approximate factors

Short-period mode	$2\zeta_{sp}\omega_{sp} = -M_q - M_{\dot\alpha} - Z_w$
	$\omega_{sp}^2 = -M_\alpha + M_qZ_w$
Dutch roll mode	$2\zeta_d\omega_d = -Y_\beta - N_r' - (L_\beta'/N_\beta')\times(N_p' - g/U_0)$
	$\omega_d^2 = N_\beta' + Y_\beta N_r'$
Roll mode	$1/T_R = -L_p' - (L_\beta'/N_\beta')(N_p' - g/U_0)$
Spiral mode	$1/T_s = T_R(g/U_0)[(L_\beta'/N_\beta')N_r' - L_r']$

approximate factors. The roots of the coupling numerator

$$\Delta_{coupl} = (s + 1/T_{N1})(s + 1/T_{N2})(s^2 + 2\zeta_N\omega_N s + \omega_N^2) \quad (5)$$

are the "zeros" of the equivalent performance function. The location of the zeros in the s plane is influenced by the magnitude and sign of the three cross-coupling derivatives $L_{\beta\alpha}'$, $N_{\beta\alpha}'$, and $M_{\beta\beta}$. This can be readily seen by rearranging Eq. (5) in two factored terms:

$$\Delta_{coupl} = s(s + 1/T_0)(s^2 + 2\zeta_0\omega_0 s + \omega_0^2) + K_N(s + 1/T_1)(s + 1/T_2) \quad (6)$$

where

$$K_N = M_{\beta\beta}(N_{\beta\alpha}'/L_{\beta\alpha}') \quad (7)$$

The coupling numerator factors of Eq. (6) are listed in Table 2.

The foregoing manipulations were applied to a slender wing configuration having appreciable aerodynamic crosscoupling in the form of the derivative $C_{l\beta\alpha}$ ($C_L = 0.3$, $U_o = 110$ m/sec, $L_{\beta\alpha}' = -62.7$ 1/sec^2, $L_{\beta\alpha}'/N_{\beta\alpha}' = -4.65$, $M_{\beta\beta} = -16.6$ 1/sec^2). Figure 2 shows the pole-zero-location of the equivalent performance function and the corresponding shape of the root loci. The variation of the characteristic roots of the aerodynamic coupled system with the steady sideslip angle β_0 is obtained by variation of the root locus gain $K(\beta_o)$. It appears that even small sideslip angles have a pronounced coupling effect on the short period and roll mode, whereas the spiral and dutch roll mode show only small but destabilizing deviations.

In order to show the strong effect of the coupling derivative $M_{\beta\beta}$ on the location of the numerator roots in the s plane, again the root locus technique can be applied. Figure 3 illustrates the numerator root loci for a second configuration, resembling a slender canard delta wing airplane ($C_L = 0.78$, $U_o = 80$ m/sec, $L_{\beta\alpha}' = -23.8$ 1/sec^2, $L_{\beta\alpha}'/N_{\beta\alpha}' = -3.57$). Equations (6) and (7) provide the direct information that the poles (0, $-1/T_o$ and ζ_o,ω_o) define the numerator roots for zero $M_{\beta\beta}$, whereas the zeros ($-1/T_1$, $-1/T_2$) are the numerator roots for infinite $M_{\beta\beta}$. The root locus gain K_N is based on the values of $L_{\beta\alpha}'/N_{\beta\alpha}'$ and $M_{\beta\beta}$.

Finally, the slender canard delta wing configuration is used as an example to illustrate in Fig. 4 the variation of the characteristic roots with the steady sideslip angle at various negative $M_{\beta\beta}$. The influence of the spiral mode has in general little effect upon the root locus and is assumed to be negligible ($1/T_2 \simeq 1/T_{N2} \simeq 1/T_s$). The zeros are readily obtained from the numerator loci of Fig. 3 which take the $M_{\beta\beta}$ effect into account. It is apparent that the ratio of the numerator frequency ω_N and the short-period frequency ω_{sp} is of importance for the sideslip sensitivity on the short-period branch, where the former frequency can be approximated by

Table 2 Coupling numerator factors

$1/T_o = -M_q$
$2\zeta_o\omega_o = -Y_\beta - N_r' + (N_{\beta\alpha}'/L_{\beta\alpha}')L_r'$
$\omega_o^2 = N_\beta' + Y_\beta N_r' - (N_{\beta\alpha}'/L_{\beta\alpha}')(L_\beta' + Y_\beta L_r')$
$1/T_1 = -L_p' + (L_{\beta\alpha}'/N_{\beta\alpha}')(N_p' - g/U_0)$
$1/T_2 = T_1 g/U_0[(L_{\beta\alpha}'/N_{\beta\alpha}')N_r' - L_r']$

the expression

$$\omega_N = (\omega_0^2 + K_N)^{1/2} \; (K_N > 0) \tag{8}$$

The sideslip sensitivity increases for large ω_N/ω_{sp} which implicate large negative values of $M_{\beta\beta}$. Similar considerations exist for the influence of the frequency ratio ω_N/ω_d on the sideslip sensitivity of the dutch roll branch, where the minimum sensitivity is obtained for $\omega_N/\omega_d \simeq 1$. In addition, the paths of the root loci are not unique as can be seen from the transition effect between the curves b and c.

Conclusions

It is the purpose of this Note to give the stability and control analyst some feel of and a simple procedure for determining aerodynamic coupling effects due to steady sideslip. On the basis of the feedback analogy, it is shown that the root locus technique is a powerful tool for inspecting and predicting the single contributions of the aerodynamic coupling derivatives on the characteristic roots for a wide variety of aircraft classes.

References

[1] Ashkenas, I. L. and McRuer, D. T., "Optimization of the Flight Control, Airframe System," *Journal of Aerospace Sciences*, March 1960, pp. 197–218.

[2] McRuer, D. T., "A Feedback-Theory Analysis of Airframe Cross-Coupling Dynamics," *Journal of Aerospace Sciences*, May 1962, pp. 525–533.

[3] Prince, L. T., "The Influence of Aeroelasticity on the Stability and Control of Airplanes and Multi-Stage Missiles," Rept. 349, April 1961, Advisory Group for Aeronautical Research and Development, Paris, France.

[4] Hamel, P., "Anwendung des Wurzelortskurvenverfahrens auf aeroelastisch gekoppelte Systeme," *Jahrbuch 1967 der WGLR*, Vieweg und Sohn, Braunschweig, Germany, 1968, pp. 350–362; translation edited by A. S. Taylor, "Application of the Root-Locus Method to Aeroelastically Coupled Systems," Library Translation 1389, June 1969, Royal Aircraft Establishment, Ministry of Technology, Farnborough, Hants., England.

[5] Porter, R. F. and Loomis, J. P., "Examination of an Aerodynamic Coupling Phenomenon," *Journal of Aircraft*, Vol. 2, No. 6, Nov.–Dec. 1965, pp. 553–556.

[6] Ulke, H., "Beiträge zur Kopplung der Längs- und Seitenbewegung von Flugzeugen," *Jahrbuch 1967 der WGLR*, Vieweg und Sohn, Braunschweig, Germany, 1968, pp. 255–270.

[7] Gersten, K. and Hummel, D., "Experimentelle und theoretische Untersuchungen über die Interferenzeinflüsse an schiebenden Flügel-Rumpf-Anordnungen mit Pfeil- und Deltaflügeln," FB 66-77, Oct. 1966, Deutsche Luft- und Raumfahrt, ZLDI, München, Germany.

Pitot Inlet Additive Drag

E. L. Crosthwait*

General Dynamics, Fort Worth, Texas

Sibulkin[1] derived the explicit analytical expression for Pitot inlet additive drag based on flow continuity and momentum considerations. However, it is difficult to apply manually at prescribed values of capture area ratio. This Note presents a unique additive drag approximation defined in simpler terms of capture area ratio, together with static pressure coefficient and total pressure coefficient ahead of the inlet.

Consider the Pitot inlet depicted in Fig. 1. The terms P_s and P_t are the upstream static and total pressures, respectively, when freestream Mach number M_0 is less than 1.0, and those pressures directly behind the normal shock when M_0 is 1.0 and greater. For a fixed M_0 and upstream capture area A_0 an approximate expression for additive drag coefficient C_{D_a} (derived intuitively) is

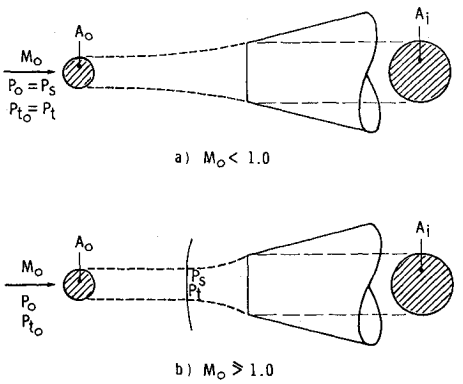

Fig. 1 Pitot inlet nomenclature.

$$C_{D_a} = C_{P_s}(1 - A_0/A_i)A_0/A_i + C_{P_t}(1 - A_0/A_i)^{(2+C_{P_s})/C_P} \tag{1}$$

where C_{D_a} = (additive drag)/$0.7P_0M_0^2A_i$, $C_{P_s} = (P_s - P_0)/0.7P_0M_0^2$, and $C_{P_t} = (P_t - P_0)/0.7P_0M_0^2$.

At $M_0 < 1.0$ (i.e., with no bow shock), $C_{P_s} = 0$ and C_{P_t} is the upstream stagnation pressure coefficient, which may be determined from the value of P_{t_0}/P_0 in standard isentropic flow tables at $M = M_0$. At $M_0 \geqslant 1.0$, C_{P_s} and C_{P_t} correspond to properties behind the normal shock and may also be determined from shock tables at $M = M_0$. Alternatively, the appropriate analytical expressions are

$$C_{P_s} = 0 \text{ at } M < 1.0 \tag{2}$$

$$C_{P_s} = \tfrac{5}{3}(M_0^2 - 1)/M_0^2 \quad \text{at} \quad M_0 \geqslant 1.0 \tag{3}$$

$$C_{P_t} = [(1 + M_0^2/5)^{3.5} - 1]/0.7M_0^2 \quad \text{at} \quad M_0 < 1.0 \tag{4}$$

$$C_{P_t} = [1.84/(1 - 1/7M_0^2)^{2.5}] - 1/0.7M_0^2 \quad \text{at} \quad M_0 \geqslant 1.0 \tag{5}$$

Numerical values from Eqs. (2–5) are shown in Fig. 2, together with values of the exponent contained in Eq. (1). At limit conditions of M_0 and capture area ratio, Eq. (1) itself has the following noteworthy properties:

$$C_{D_a} = (1 - A_0/A_i)^2 \quad \text{at} \quad M_0 = 0 \tag{6}$$

$$C_{D_a} = C_{P_t} \quad \text{at} \quad A_0/A_i = 0 \tag{7}$$

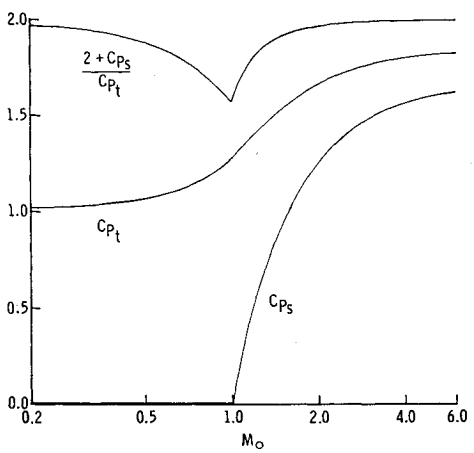

Fig. 2 Static and total pressure coefficients.

Received August 11, 1970.

* Deign Specialist.